BL-9C/2023G163

Local Structural Analysis of Subnano Copper Oxide Particles for Low Temperature Methane Activation

Kazutaka SONOBE[1], Makoto TANABE[2]* and Kimihisa YAMAMOTO[1]
[1] Laboratory for Chemistry and Life Science, Institute of Innovative Research and JST−ERATO, Yamamoto Atom Hybrid Project, Tokyo Institute of Technology, Yokohama 226-8503, Japan
[2] Integrated Center for Science and Humanities, Fukushima Medical University, Fukushima 960-1295, Japan

1 Introduction

Subnanostructured particles (SNPs) exhibit drastic enhancement of reactivity, which are approximately 1 nm in size. The reactivity of SNPs has often been realized as the activation of small inert molecules in enzymic systems [1]. One method to synthesize size-controlled SNPs was the use of macromolecule cage materials. Dendritic phenyl azomethine (DPA) is the macromolecule cage with a rigid structure and nitrogen-containing ligands, which leads to less steric hindrance and accumulation of a precise number of metal atoms [2]. The atom-specific noble-metal SNPs have been reported to show high catalytic performance in hydrocarbon oxidation using O_2 molecules [3]. Non-noble-metal oxide SNPs exhibit enhanced catalytic performance because of the activation of metal–oxygen bonds or the formation of structural defects on their surface as the size of the SNPs is reduced [4,5].

Copper-containing SNPs are especially attracted, because copper is expected to generate strong active sites at low temperatures for selective methane oxidations such as methane mono-oxygenase in methanotrophs. Heterogeneous copper oxide clusters loaded in cage materials have successfully achieved methane activations, such as copper loaded zeolite or metal-organic frameworks. In the catalysis using cage materials, the significance of ligand or cage effects has been claimed in low-temperature methane oxidation on copper-containing SNPs [6]. However, the reactivity of such a subnano copper particles without any protective ligands for reaction temperature has not been discussed in experimental heterogeneous reactions. Herein, we report on the structural properties of nonfunctionalized copper SNPs with the potential to cause low-temperature methane activation.

2 Experiment

Preparation of copper oxide SNPs. The synthetic scheme of copper oxide SNPs was described in Fig. 1A. In a glovebox, $CHCl_3$ was added to the solution of the $CuCl_2$ powder, and then the solution was sonicated for 10 min. To the solution, DPA was added and stirred for 1 h. Three equivalents of $NaBEt_3H$ to the mole amount of copper in the $CuCl_2$-DPA complex were added with vigorous stirring. The solution containing the copper SNPs was exposed to air, giving the oxidized copper SNPs covered with DPA. The reaction mixture was added to a separating funnel and water was also poured into the same vessel. The copper oxide SNPs were extracted with water and the DPA remained in the organic solvent layer. The aqueous solution containing the separated SNPs was added dropwise into the dispersed suspension containing SiO_2 in water. The solvent was evaporated, providing the copper SNPs loaded on silica.

A high-angle annular dark-field scanning transmission electron microscopy (HAADF-STEM) image and the particle size distribution of the copper oxide SNPs are shown in Figs 1C and D. The observed average particle diameter was estimated about 0.9 nm. Separation of the copper SNPs from the DPA template was confirmed by Fourier transform infrared spectroscopy (FT-IR). The copper SNPs on silica showed two unique broad peaks at 1020 and 972 cm^{-1}, which were assigned as a deformation vibration of the Cu−O−H bond (Fig. 1E). These results indicate that the copper oxide SNPs are completely extracted from water with separation from the organic DPA template.

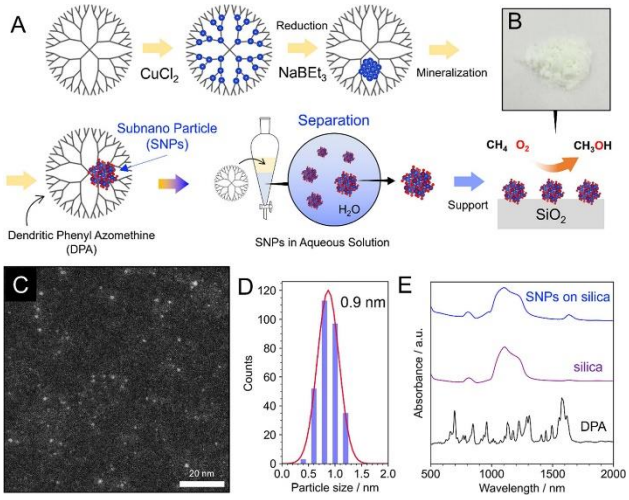

Fig 1. (A) Schematic illustration of the separation of copper oxide SNPs from the DPA ligand. (B) Photograph of SNPs supported on silica. (C) HAADF-STEM micrograph of copper oxide SNPs cast on a carbon film grid from aqueous solution. (D) Particle size distribution estimated from the HAADF-STEM image. (E) FT-IR spectra of SNPs, SNPs on silica, silica, and the DPA template. The SNP peaks were obtained from the difference spectrum of SNPs on silica and the silica support.

X-ray Absorption Spectroscopic Analysis. XAFS spectra were measured in transmission mode at 180s for each scan. The sample of 50 mg was pelletized in a metal

ring and placed into a custom-designed and heat-resistant cell. The *in situ* experiment of copper reduction by methane was conducted in CH_4 gas flow (30 sccm) in 373 K in Quick XAFS (QXAFS) mode. The experiment of autoreduction was conducted in a He gas flow (30 sccm) from ambient temperature to 673 K in QXAFS mode. The XAFS analyses were carried out using Athena in Demeter. The curve of k^3-weighted EXAFS spectra and Fourier-transformed EXAFS (FT-EXAFS) spectra was curve-fitted using the Larch program. The Fourier-transformed range (k = 3−12 A^{-1}) and Fourier Filtered range (R = 1−4 A) were used for curve fitting. The theoretical amplitude and phase shift for curve fitting were obtained from FEFF 8.5 calculations. The simulations of FT-EXAFS were based on theoretical FEFF calculations conducted by the Larch program. The wavelet transform of EXAFS was also carried out by the Larch program.

3 Results and Discussion

The reduction of the copper oxide SNPs under methane gas flow in the same reaction also supported the methane oxidation on copper oxide SNPs. The Cu−K edge X-ray absorption near-edge structure (XANES) revealed a pre-edge peak at 8978 eV, which was assigned as Cu(II). The edge peak at 8982 eV increases in methane flow at 373 K, characteristic of Cu(I), and significant reduction of the Cu(II) species was confirmed by the oxidations of methane on the copper oxide SNPs (Fig. 2).

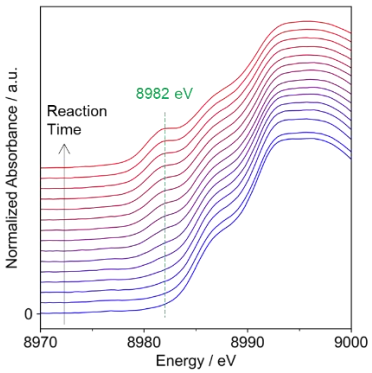

Fig. 2. *In situ* Cu K edge XANES spectra of copper oxide SNPs on silica under CH_4 gas flow in 373 K. The green line at 8982 eV shows a peak position of characteristic edge peak for Cu(I).

The local atomic configurations of the SNPs cannot be assigned on the basis of the crystal structures of copper oxide and hydroxide. The Fourier-transformed extended X-ray absorption fine structure (FT-EXAFS) of the SNPs shows specific atomic radial distances in two overlapped peaks (2.04 and 2.48 A) and a small peak around 3.1−3.7 A (Fig. 3A). The overlapped peaks are regarded as Cu−O bond distances, and the long and short Cu−O bonds are displayed as independent components in the wavelet-transformed EXAFS (Fig. 3B). The long distance is assigned to a Jahn−Teller strain. The FT-EXAFS peaks of tenorite (CuO) and cuprite (Cu_2O) (Fig. 3A) are not in agreement with this long Cu−O distance. The FT-EXAFS intensity of spertiniite ($Cu(OH)_2$) is also not in agreement with the long Cu−O peaks. The other copper mineral phase was potentially assigned as the structure of the SNPs. The atacamite $Cu_2(OH)_3Cl$ structure is also known as a stable copper phase with local structures (Figs. 3C−E) including the Jahn−Teller strain (Fig. 3D). However, the Cu−Cl peak of the atacamite local structure is not observed in the FT-EXAFS of the SNPs, and the coordination number of long Cu−O peaks is larger than the Jahn−Teller strained Cu−O coordination number in atacamite. This suggests that the local structures of the copper SNPs are close to those of atacamite, where the chloride ions may be replaced with hydroxide ions in a water extraction process.

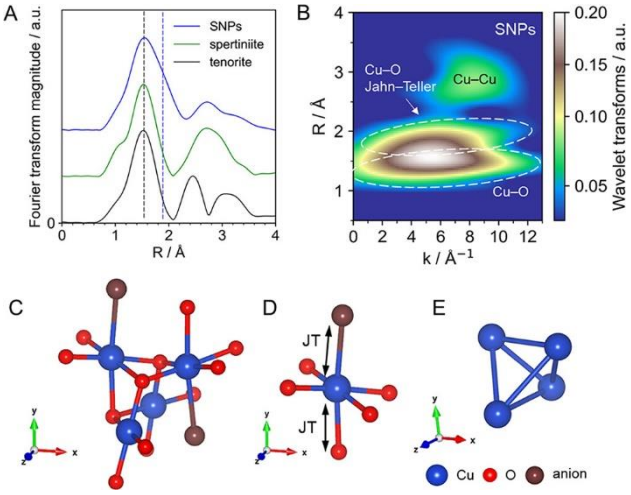

Fig. 3. (A) Radial distribution functions from FT-EXAFS of the copper oxide SNPs on silica, spertiniite, and tenorite. The blue and black dashed lines displayed the peak positions of long and short Cu–O distance. (B) Wavelet-transformed EXAFS of the copper SNPs. (C) Local structure of atacamite ($Cu_2(OH)_3Cl$). (D) Structure of the first coordination sphere of atacamite with a Jahn–Teller (JT) distortion; the distorted and elongated Cu–O and Cu–Cl are indicated by black arrows. (E) Tetrahedral coordination of four copper atoms in the structure of panel "C".

The elementary reduction of copper SNPs possibly involves a mechanism for the generation of bis-dicopper μ-oxo dicopper cores. The $Cu_2(\mu\text{−}O)_2$ cores were reported to be generated by the addition of molecular oxygen to the oxygen vacancy of Cu(I) dimers. The generation of Cu(I) species under nonreductive conditions was also observed from in situ XANES spectral measurements (Fig. 4A). The pre-edge peak intensity at 8978 eV was attributed to the 1s-3dp transition of Cu(II), and the edge peak at 8982 eV characteristic of Cu(I) was increased with the temperature. The results indicated the spontaneous reduction of copper SNPs from ambient temperature, which has been known as autoreduction. Autoreduction is the disproportionation of metal oxide to the reduced metal and spin triplet molecular oxygen. The reduction temperature of the subnano copper particles was lower than that reported for other copper cluster compounds. The structural transformation of the copper oxide SNPs was observed by *in situ* XAFS

measurements with heating from 297 to 673 K in a He flow. The local atomic configurations analyzed by FT-EXAFS indicated Cu−O bond elongation (Fig. 4B). This major component of the Cu−O bonds was changed from a short Cu−O bond to a Jahn−Teller distorted bond with heating (Fig. 3D). The Cu−Cu distance was almost maintained in the observed temperature range. The results suggest the desorption of oxygen from a short Cu−O site, and the oxygen defects may induce the generation of $Cu_2(\mu{-}O)_2$ cores. The structural change in subnano size at low temperature can accelerate methane conversion under mild conditions, and this effect may potentially have been underestimated in industrial catalysts to date.

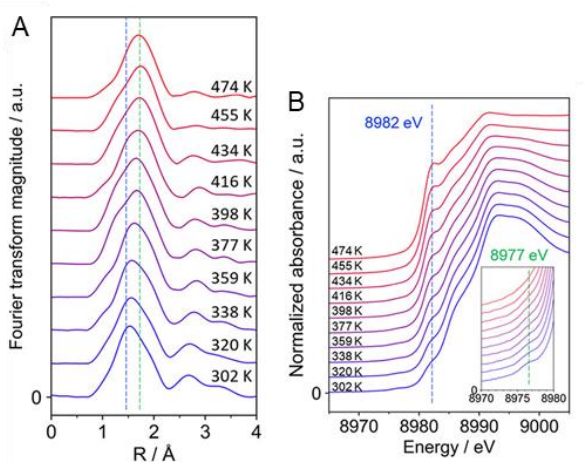

Fig. 4. (A) Radial distribution functions of the FT-EXAFS spectra of the SNPs on silica with helium flow at 302–474 K. The blue and green lines show the positions of short and long Cu–O peaks. (B) *In situ* Cu K-edge XANES of the SNPs on silica with helium flow at 302–474 K.

4 Conclusion

We have observed that subnanosized copper oxides showed high reactivity for methane oxidation due to the structural effects of the naked copper SNPs. The mineralized local structures induce the generation of active oxygen species by their atomic configurations. The generation of active oxygen species is a significant initial step for all oxidation reactions. Our discovery of the specific copper oxide structure in a subnano-ordered scale might occur in other metal oxide particles, and this effect may be one reason why the catalytic activity is often enhanced. These results have the potential to provide inspiration for nanostructured catalysis or efficient resource utilization in the conversion of inert molecules such as methane.

Acknowledgement

The authors thank Prof W.-J Chun (ICU) and Prof. T. Imaoka (Tokyo Tech.) for helpful discussion about XAFS measurements. The XAFS measurements were conducted at the BL-9C beamlines of the High Energy Accelerator Research Organization Institute of Materials Structure Science Photon Factory (KEK-IMSS-PF) under the approval of the Photon Factory Advisory.

References

[1] M. F. Hochella Jr. *et al*., *Science* **363**, 1414 (2019).
[2] K. Yamamoto *et al*., *Chem. Rev.* **120**, 1397 (2020).
[3] M. Huda, K. Yamamoto *et al.*, *Angew. Chem., Int. Ed.*, **58**, 1002 (2019).
[4] K. Sonobe, K. Yamamoto, *et al.*, *ACS Nano*, **14**, 1804 (2020).
[5] K. Sonobe, K. Yamamoto, *et al.*, *Chem. Eur. J.* **27**, 8452 (2021).
[6] P. H. Walton, *et al.*, *Nat. Catal.* **1**, 571 (2018).

Research Achievements

1. Kazutaka Sonobe, Makoto Tanabe, Takane Imaoka, Wang-Jae Chun, Yumi Ida, Akiyoshi Kuzume, and Kimihisa Yamamoto, "Non-Functionalized Subnanometer Copper Nanoparticles for Low-Temperature Methane Activation", *ACS Appl. Nano Mater.*, 7, 5802 (2024). The cover picture was selected.
   https://doi.org/10.1021/acsanm.3c04281

* m-tanabe@fmu.acjp